ANNALS OF
BOTANY
Founded 1887

PART OF A SPECIAL ISSUE ON FLOWER DEVELOPMENT

AGO1 controls arabidopsis inflorescence architecture possibly by regulating *TFL1* expression

P. Fernández-Nohales[1,†], M. J. Domenech[1], A. E. Martínez de Alba[2], J. L. Micol[3], M. R. Ponce[3] and F. Madueño[1,*]

[1]*Instituto de Biología Molecular y Celular de Plantas, Consejo Superior de Investigaciones Científicas-Universidad Politécnica de Valencia, Valencia 46022, Spain,* [2]*Institut Jean-Pierre Bourgin, UMR 1318, INRA, Route de St-Cyr, 78000 Versailles, France and* [3]*Instituto de Bioingeniería, Universidad Miguel Hernández, Campus de Elche, 03202 Elche, Alicante, Spain*
[†]*Present address: Centre for Research in Agricultural Genomics, CSIC-IRTA-UAB-UB, 08193 Barcelona, Spain.*
* For correspondence. E-mail madueno@ibmcp.upv.es

• **Background and Aims** The *TERMINAL FLOWER 1* (*TFL1*) gene is pivotal in the control of inflorescence architecture in arabidopsis. Thus, *tfl1* mutants flower early and have a very short inflorescence phase, while *TFL1*-overexpressing plants have extended vegetative and inflorescence phases, producing many coflorescences. *TFL1* is expressed in the shoot meristems, never in the flowers. In the inflorescence apex, TFL1 keeps the floral genes *LEAFY* (*LFY*) and *APETALA1* (*AP1*) restricted to the flower, while LFY and AP1 restrict *TFL1* to the inflorescence meristem. In spite of the central role of *TFL1* in inflorescence architecture, regulation of its expression is poorly understood. This study aims to expand the understanding of inflorescence development by identifying and studying novel *TFL1* regulators.
• **Methods** Mutagenesis of an *Arabidopsis thaliana* line carrying a *TFL1::GUS* (*β-glucuronidase*) reporter construct was used to isolate a mutant with altered *TFL1* expression. The mutated gene was identified by positional cloning. Expression of *TFL1* and *TFL1::GUS* was analysed by real-time PCR and histochemical GUS detection. Double-mutant analysis was used to assess the contribution of *TFL1* to the inflorescence mutant phenotype.
• **Key Results** A mutant with both an increased number of coflorescences and high and ectopic *TFL1* expression was isolated. Cloning of the mutated gene showed that both phenotypes were caused by a mutation in the *ARGONAUTE1* (*AGO1*) gene, which encodes a key component of the RNA silencing machinery. Analysis of another *ago1* allele indicated that the proliferation of coflorescences and ectopic *TFL1* expression phenotypes are not allele specific. The increased number of coflorescences is suppressed in *ago1 tfl1* double mutants.
• **Conclusions** The results identify AGO1 as a repressor of *TFL1* expression. Moreover, they reveal a novel role for AGO1 in inflorescence development, controlling the production of coflorescences. AGO1 seems to play this role through regulating *TFL1* expression.

Key words: Flower development, *TERMINAL FLOWER 1*, *TFL1*, *ARGONAUTE1*, *AGO1*, plant architecture, inflorescence architecture, flowering, *Arabidopsis thaliana*.

INTRODUCTION

The architecture of the aerial part of a plant depends on the number, size, shape and position of its leaves, shoots and flowers (Benlloch *et al.*, 2007). All these organs derive from the shoot apical meristem (SAM), a small group of stem cells located at the shoot apex (Bowman, 1994; Wolpert and Tickle, 2010). After germination, the SAM is a vegetative meristem that produces leaves and branches. When endogenous and environmental conditions are appropriate, transition to the flowering phase takes place and the SAM is transformed into an inflorescence meristem, which produces flowers (Amasino 2010; Huijser and Schmid, 2011; Andrés and Coupland, 2012).

In *Arabidopsis thaliana* (hereafter, arabidopsis), during the vegetative phase, the SAM produces leaves on its flanks without internode elongation, which leads to the formation of a rosette (Figs 1C and 5A, E). In contrast, internodes formed after the floral transition do elongate, leading to the formation of the main inflorescence, where two phases can be distinguished. During the first inflorescence phase (I1), the SAM produces cauline leaves on its flanks which subtend axillary lateral inflorescences, called coflorescences; in the second inflorescence phase (I2), the SAM produces flowers without subtending leaves (Ratcliffe *et al.*, 1998) (Figs 1C and 5A, E). The arabidopsis inflorescence is an open raceme, where the flowers are formed only on the flanks of the inflorescence SAM, which has indeterminate growth and never develops into a flower (Alvarez *et al.*, 1992; Weberling, 1992; Prusinkiewicz *et al.*, 2007).

This inflorescence architecture is based on the antagonistic action of two sets of genes that are expressed in distinct non-overlapping domains of the inflorescence apex. On the one hand, the main floral meristem identity genes *LEAFY* (*LFY*) and *APETALA1* (*AP1*), which encode transcription factors, are expressed in the primordia formed at the flanks of the inflorescence SAM, conferring to these primordia the identity of floral meristems, as deduced from the fact that loss of function of these genes causes replacement of flowers by inflorescence-like structures (Mandel *et al.*, 1992; Weigel *et al.*, 1992; Blázquez *et al.*, 2006). On the other hand, the shoot/inflorescence identity gene *TERMINAL FLOWER 1* (*TFL1*) shows strong expression in
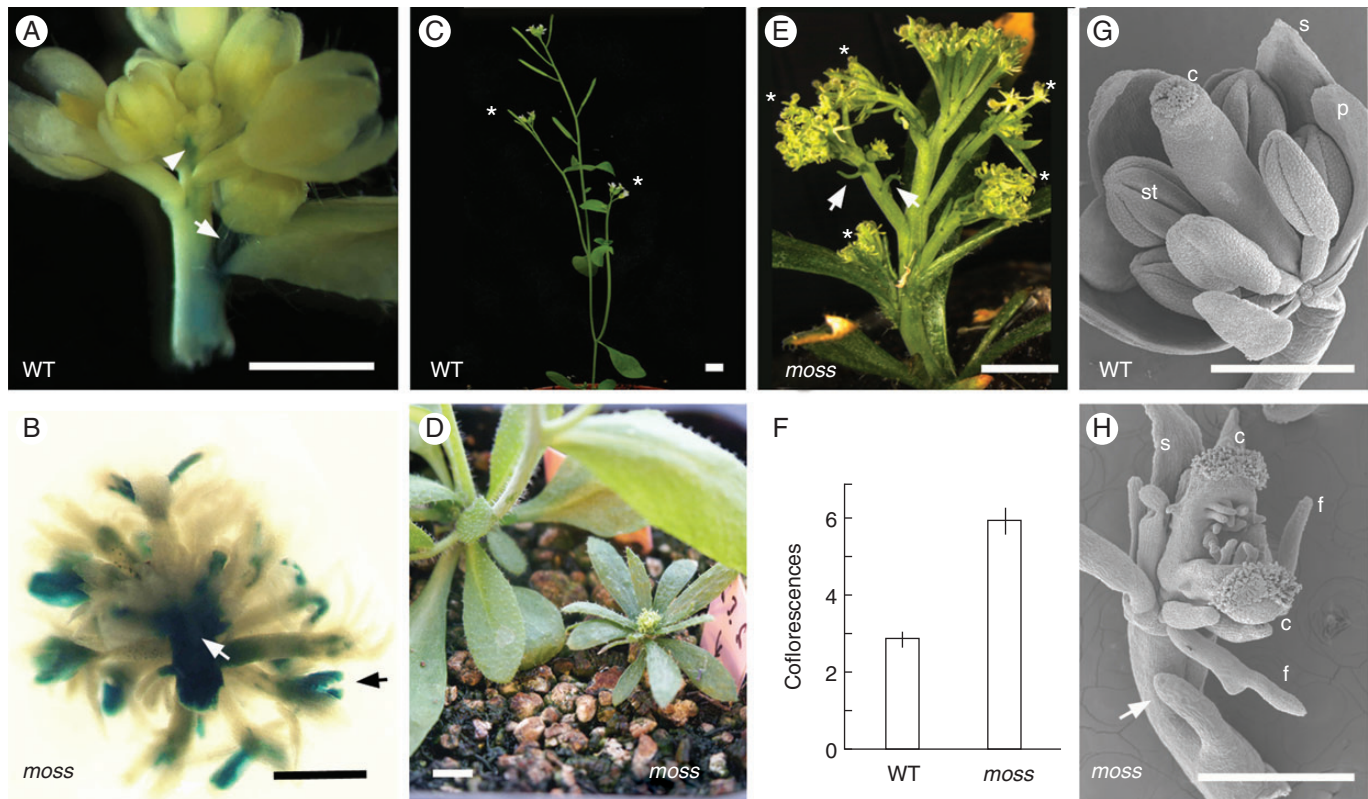
Fɪɢ. 1. Phenotype of the *moss* mutant. (A) Expression pattern of *TFL1::GUS* in a bolting inflorescence apex of a wild-type (WT) parental plant. GUS signal is observed in the inflorescence meristem (arrowhead) and the inflorescence stem; a strong signal is seen in the stem of a developing coflorescence (arrow). GUS signal is not detected in flowers. (B) Expression pattern of *TFL1::GUS* in the main inflorescence of a *moss* plant. GUS signal is apparent in flowers (black arrow) and in the inflorescence stem (white arrow). (C) WT plant with two coflorescences (asterisks) in the main inflorescence stem. (D) A *moss* plant (right) beside a WT plant (left). (E) Inflorescence of a mature *moss* plant with five coflorescences (asterisks) in the main inflorescence stem. There is no elongation of the internodes between flowers. The presence of filamentous organs (arrows) in a coflorescence stem is observed. (F) Histogram showing the number of coflorescences in the main inflorescence stem of WT and *moss* plants. Values correspond to the average of 15 plants $\pm$ standard error. (G) Scanning electron microscopy (SEM) of a WT flower, showing the different floral organs. (H) SEM of a *moss* flower. A filamentous organ (arrow) is present in the pedicel; petals and stamens are replaced by filaments; and the carpels are unfused and ovules are exposed. Abbreviations: c, carpel; f, filament; p, petal; s, sepal; st, stamen. Scale bars: 5 mm in (A-E); 500 μm in (G) and (H).

the centre of the SAM of the main and lateral inflorescences (Bradley *et al.*, 1997; Conti and Bradley, 2007) (Fig. 1A). Expression of *TFL1* is required for the identity of these meristems, and loss of *TFL1* function leads to the conversion of these inflorescence meristems into floral meristems, so that in *tfl1* mutants the lateral coflorescences are replaced by axillary flowers and the main inflorescence shoot exhibits determinate growth, ending in a terminal flower (Shannon and Meeks-Wagner, 1991; Alvarez *et al.*, 1992; Bradley *et al.*, 1997). The complementary expression pattern of these two types of genes is, therefore, required for the architecture of arabidopsis inflorescence, where the SAM remains indeterminate and the flowers are formed at its flanks (Blázquez *et al.*, 2006; Benlloch *et al.*, 2007; Teo *et al.*, 2013). This expression pattern is maintained by mutual repression between *TFL1* and the floral meristem identity genes, and, in the absence of TFL1 function, in *tfl1* mutants, *LFY* and *AP1* expression invades the inflorescence meristems, correlating with the conversion of these meristems into floral meristems (Bradley *et al.*, 1997; Liljegren *et al.*, 1999; Ratcliffe *et al.*, 1999; Ferrándiz *et al.*, 2000).

TERMINAL FLOWER 1 not only controls determination of the inflorescence apex but it also regulates the length of the different developmental phases that the SAM goes through

(Ratcliffe *et al.*, 1998). In fact, TFL1 acts as a repressor of the transition to flowering, as shown by the fact that the vegetative phase in *tfl1* mutants is shorter than in the wild type (Bradley *et al.*, 1997; Ratcliffe *et al.*, 1998). Conversely, constitutive expression of *TFL1* in *35S::TFL1* plants causes late flowering and an enlargement of the I1 phase, with increased production of coflorescences (Ratcliffe *et al.*, 1998). This role of TFL1 in controlling the transition to flowering correlates with its expression, at a low level, in the vegetative SAM (Bradley *et al.*, 1997), and is thought to be mediated by its activity as a transcriptional co-repressor through its interaction with the bZIP-type transcription factor FD (Hanano and Goto, 2011). Possibly, TFL1 also repress flowering by interfering with the activity of FLOWERING LOCUS T (FT), a strong flowering promoter. FT is a homologous protein to TFL1, which also acts in a transcriptional complex with FD (Abe *et al.*, 2005; Wigge *et al.*, 2005), and TFL1 and FT have been suggested to compete for protein partners (Hanzawa *et al.*, 2005; Ahn *et al.*, 2006; Ho and Weigel, 2014).

In summary, the pattern of *TFL1* expression seems pivotal to its function: it is weak in the vegetative SAM and upregulated with the floral transition, after which *TFL1* is expressed strongly in the inflorescence SAM and also throughout the inflorescence

stem (Bradley *et al.*, 1997; Conti and Bradley, 2007). How this dynamic complex expression pattern is established and maintained is still poorly understood. Transcriptional repression of *TFL1* in the floral meristem is the only well-known aspect of that question. On the one hand, multiple molecular genetic evidence indicates that the AP1 and LFY transcription factors act in the flower as repressors of *TFL1* (Liljegren *et al.*, 1999; Ratcliffe *et al.*, 1999; Ferrándiz *et al.*, 2000; Parcy *et al.*, 2002). Recent support for this hypothesis has been provided by the demonstration of direct binding of AP1 and LFY to the 3′ region of the *TFL1* gene (Kaufmann *et al.*, 2010; Moyroud *et al.*, 2011; Winter *et al.*, 2011). In addition, a recent study has shown that SUPPRESSOR OF OVER-EXPRESSION OF CONSTANS 1 (SOC1), SHORT VEGETATIVE PHASE (SVP), AGAMOUS-LIKE 24 (AGL24) and SEPALLATA 4 (SEP4), from the MADS-box transcription factor family (like AP1), also contribute, acting redundantly and directly, to suppress *TFL1* in the developing flower, and are essential for the repression of *TFL1* by LFY and AP1 (Liu *et al.*, 2013).

In addition to regulation through transcription factors, other transcriptional or post-transcriptional mechanisms might contribute to controlling the expression pattern of the *TFL1* mRNA. One of these is RNA-mediated silencing, or RNA silencing, which is a central mechanism of gene regulation in eukaryotes (Carthew and Sontheimer, 2009). RNA silencing relies on ARGONAUTE (AGO) proteins, which constitute the core of the RNA-induced silencing complexes (RISCs), where they associate with distinct types of small RNAs that guide them to their targets through complementary base pairing (Baulcombe, 2004; Vaucheret, 2006; Bartel, 2009; Brodersen and Voinnet, 2009). In arabidopsis, AGO1 is the effector and pivotal component of RISCs that associate with microRNAs (miRNAs) and mediate post-transcriptional gene silencing (Vaucheret *et al.*, 2004; Baumberger and Baulcombe, 2005; Qi *et al.*, 2005). Characterization of *ago1* mutants, which exhibit strong pleiotropic morphological phenotypes, shows that AGO1 contributes to the regulation of a wide variety of central developmental processes (Bohmert *et al.*, 1998; Kidner and Martienssen, 2005*a*; Smith *et al.*, 2009; Jover-Gil *et al.*, 2012; Ji *et al.*, 2013).

With the aim of identifying novel regulators of *TFL1* expression, we carried out a genetic screening for mutants with altered *TFL1* expression, making use of an arabidopsis reporter line containing a *TFL1::GUS* (*β-glucuronidase*) reporter transgene. We isolated a mutant with severe alterations in both *TFL1* expression and inflorescence architecture, and found that a mutation in the *AGO1* gene caused both phenotypes. Our results reveal a novel role for AGO1 in the control of inflorescence architecture, possibly through regulation of the expression of *TFL1*.

MATERIALS AND METHODS

Plant material and growth conditions

Arabidopsis thaliana plants were grown in a 1:1:1 mixture of sphagnum:perlite:vermiculite, at 21 °C under long-day photoperiods (16 h light), in growth cabinets, illuminated by cool-white fluorescent lamps (150 μE m^{-2} s^{-1}). For the mutagenesis and the mutant screening, plants were grown in the greenhouse at 21 °C and long-day photoperiods, which were maintained with supplementary lighting [400 W Philips HDK/400 HPI (R) (N)].

The reporter L*er* pBTG1 arabidopsis line used as the parent for the mutagenesis, and the *moss/ago1-103*, *ago1-52* (Jover-Gil *et al.*, 2012) and *tfl1-2* (Alvarez *et al.*, 1992) mutants were from the Landsberg *erecta* (L*er*) genetic background. The *ago1-26* (Morel *et al.*, 2002) and *tfl1-1* (Shannon and Meeks-Wagner, 1991) mutants were from the Columbia (Col) genetic background. *ago1-26* was kindly provided by H. Vaucheret (INRA, Versailles, France).

The *moss/ago103* mutant was backcrossed three times to L*er* before being used for the experiments described here.

TFL1::GUS reporter constructs

The arabidopsis L*er* pBTG1 line used as the parent for the mutagenesis was homozygous for the *TFL1::GUS* reporter construct pBTG1. All plants shown in Figs 2 and 4 were homozygous for the *TFL1::GUS* reporter construct pBTG6.

The pBTG1 construct was obtained by sub-cloning into the pBIN19 binary vector (Bevan, 1984) of a DNA fragment containing the *GUS* gene from the pBI121 vector (Jefferson *et al.*, 1987) flanked by the complete 5′ intergenic region (2172 bp) and by a fragment of the 3′ intergenic region [2722 bp, starting downstream of the 3′-untranslated region (UTR)] of the L*er* *TFL1* gene (Supplementary Data Fig. S1). The 5′ and 3′ intergenic fragments in pBTG1 were amplified by PCR from a genomic clone from the *TFL1* L*er* gene, with the TFL15′intF and TFL15′intR primers, which add *Sal*I and *Bam*HI restriction sites, respectively, to the 5′ intergenic fragment, and with the TFL13′2.7F and TFL13′2.7R primers, which add *Sac*I/*Xba*I and *Eco*RI/*Kpn*I restriction sites, respectively, to the 2722 bp 3′ intergenic fragment (Supplementary Data Table S1). The pBTG6 construct was kindly provided by A. Serrano-Mislata and is identical to pBTG1 except that the *TFL1* 3′ intergenic region is a 4667 bp fragment with the complete 3′ intergenic region (starting after the stop codon of the *TFL1* coding sequence; Supplementary Data Fig. S1; A. Serrano-Mislata and F. Madueño, IBMCP, Valencia, Spain, unpubl. res.). An equivalent *TFL1* genomic construct, containing the same 5′ and 3′ intergenic regions as those in pBTG6, fully rescued the *tfl1-1* mutant phenotype (Sohn *et al.*, 2007; Kaufmann *et al.*, 2010).

Mutagenesis, mutant screening and genetic analysis

Seeds from the L*er* pBTG1 line were mutagenized with ethyl methanesulfonate (EMS; Weigel and Glazebrook, 2002), and 1850 M_2 families, harvested from individual M_1, plants were generated. For the mutant screening, 25 plants from each M_2 family were grown in the greenhouse. After about 3 weeks of growth, the main inflorescence apices from these M_2 plants were dissected and subjected to GUS staining. Plants with alterations in both the *TFL1::GUS* expression pattern and inflorescence architecture were retained for subsequent analysis.

Mapping and cloning of the moss/ago1-103 mutation

Low-resolution mapping of the *moss* mutation was performed as previously described (Ponce *et al.*, 2006). In brief, the DNA of 50 F_2 phenotypically mutant plants was individually

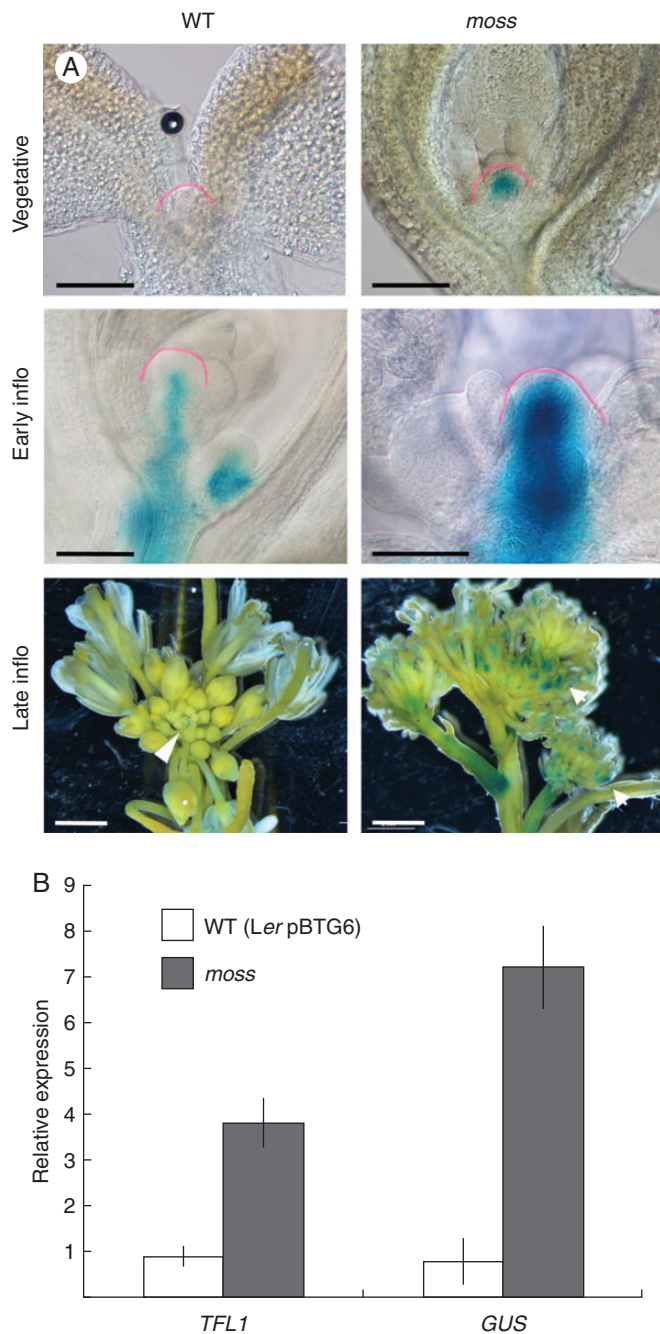WT   *moss*

Vegetative

Early inflo

Late inflo

B

Fig. 2. Effect of the *moss* mutation on the expression of *TFL1*. (A) Expression of *TFL1::GUS* in wild-type (WT) and *moss* shoot apices in different developmental stages. Apices from plants at equivalent developmental stages were compared. In late inflorescences, GUS signal in the WT apex is restricted to the inflorescence meristem (arrowhead), while in the *moss* apex signal is also observed in the flowers (arrows). The SAM in the vegetative and early inflorescence apices is outlined with a pink line. (B) mRNA levels of *TFL1* and *GUS* in the inflorescence apices of WT (L*er* pBTG6) and *moss* plants, determined by RT-qPCR. Samples were from main inflorescence apices from 40-day-old plants (= late inflorescence). The mRNA level of the *UBIQUITIN 10* gene was used as reference. Values represent the means of three technical replicates ± standard error. Scale bars: 300 μm in vegetative and early inflorescence apices; 2 mm in late inflorescence apices.

extracted and used as a template to multiplex PCR co-amplify 32 simple sequence length polymorphism (SSLP) and insertion/deletion (In/Del) molecular markers using fluorescently labelled

oligonucleotides as primers. For fine mapping, 421 F_2 plants were used to assess iteratively linkage between *moss* and molecular markers designed according to the polymorphisms between L*er* and Col-0 described at the Monsanto Arabidopsis Polymorphism Collection database (http://www.arabidopsis.org).

For sequencing of the *moss* allele, PCR products spanning the *AGO1* transcriptional units were obtained using the oligonucleotide primers described in Jover-Gil *et al.* (2012) and as templates genomic DNA from L*er* and from three different *moss* mutant plants. The sequences of the *AGO1* gene obtained from the three *moss* plants were identical.

Genetic combinations

Homozygous single mutants were cross-fertilized, and double mutants were identified among the F_2 segregants by novel phenotypes and confirmed by genotyping and/or by segregation of F_3 progeny. Genotyping of the *moss/ago1-103* mutation was performed with a derived cleaved amplified polymorphic sequence (dCAPS) marker with the primers dCAPmoss-Fw and dCAPmoss-Rv (see Supplementary Data Table S1), which, when followed by digestion with *Xba*I, generated a single fragment of 237 bp in the wild-type allele or two fragments of 210 and 27 bp in the mutant. Genotyping of the *ago1-52* mutation (Jover-Gil *et al.*, 2012) was performed by sequencing the genomic region amplified by primers AGOF8 and AGOR6 (Supplementary Data Table S1). Genotyping of the *ago1-26* mutation (Morel *et al.*, 2002) was performed by sequencing the genomic region amplified by primers AGOF1 and AGOR8 (Supplementary Data Table S1).

Histochemical detection detection of GUS activity

Tissue samples from Figs 1 and 4 were incubated for 8 h at 37 °C with medium astringency staining buffer (50 mM sodium phosphate, 2 mM ferrocyanide, 2 mM ferricyanide, 0·2 % Triton X-100 and 1 mM X-Gluc). Samples from Fig. 2 were incubated for 4 h at 37 °C with astringency staining buffer (50 mM sodium phosphate, 10 mM ferrocyanide, 10 mM ferricyanide, 0·2 % Triton X-100 and 1 mM X-Gluc). Following staining, plant material was incubated for 30 min in fixation solution [50 % ethanol (v/v), 10 % acetic acid (v/v), 5 % formaldehyde (w/v)], and cleared in chloralhydrate solution [72 % chloralhydrate (v/v) and 11 % glycerol (w/v)] All the plants used in the assays were homozygous for the *TFL1::GUS* reporter transgene.

Scanning electron microscopy (SEM)

Samples were vacuum infiltrated with 4 % formaldehyde (w/v) in 1× phosphate-buffered saline (PBS) for 10 min and fixed with fresh solution for 16 h at 4 °C. Samples were dehydrated in an ethanol series and critical point dried in liquid CO_2 (Polaron E300 apparatus). Dried samples were mounted on stubs. Then, samples were coated with gold-palladium (4:1) in a Sputter Coater SCD005 (Baltec). Scanning electron microscopy was performed with a Jeol JSM-5410 microscope (10 kV).

Expression analyses

For quantitative PCR (RT-qPCR), 2000ng of total RNA, extracted with the RNeasy Plant Mini Kit (Qiagen), were treated with DNase (DNA-free kit, AmbioN) and used for

cDNA synthesis, performed with the SuperScriptII cDNA synthesis kit (Invitrogen). The qPCR mix was prepared in a final volume of 20 μL containing 1200 ng of the cDNA, $1\times$ Power SYBR Green master mix (Applied Biosystems) and 300 nM primers. Primers used to amplify the GUS and TFL1 cDNAs were: GUS-Fw and GUS-Rv for *GUS*, and TFL1-Fw and TFL1-Rv for *TFL1* (Supplementary Data Table S1). Results were normalized to the expression of the UBQ10 gene (Czechowski *et al.*, 2005), with the primers UBQ-Fw and UBQ-Rv (Supplementary Data Table S1). The PCRs were run and analysed using the ABI PRISM 7700 (Applied Biosystems) sequence detection system. The obtained data were treated according to Schmittgen and Livak (2008).

Sequence analysis

The search for miRNA target sites in the *TFL1* mRNA sequence was carried out using different online databases (Griffiths-Jones, 2004; Rusinov *et al.*, 2005; Griffiths-Jones *et al.*, 2006, 2008; Kozomara and Griffiths-Jones, 2014).

RESULTS

Isolation of the arabidopsis moss *mutant*

To identify regulators of the expression of the arabidopsis *TFL1* gene, we screened an M_2 mutant population derived from L*er* pBTG1 M_1 plants treated with EMS. The L*er* pBTG1 line was generated by transformation of L*er* with a *TFL1::GUS* reporter construct where the *GUS* gene is flanked by the complete 5′ intergenic region (approx. 2·2 kb) and approx. 2·7 kb of the 3′ intergenic region of *TFL1* (Supplementary Data Fig. S1). In L*er* pBTG1, *GUS* expression essentially reproduces the expression pattern of the endogenous *TFL1* gene. In L*er* pBTG1 bolting inflorescences, a strong GUS signal was detected in the apical inflorescence meristem, and in young coflorescence buds, but it was absent from flowers (Fig. 1A). Because *TFL1* is a regulator of plant and inflorescence architecture, we selected plants exhibiting both an altered *TFL1::GUS* pattern and altered plant architecture.

In the screening, we identified an M_2 family including mutant plants with a phenotype characterized by abnormal *TFL1::GUS* expression, which was strong in the inflorescence stem and ectopic in flowers, and also by a dramatically modified plant and inflorescence architecture (Fig. 1B, D, E). These plants were sterile, and in the progeny of some M_2 fertile siblings from that family the phenotype segregated in a 1:3 proportion, indicating that this was due to recessive mutation(s) in a single locus. These mutant plants were very small (Fig 1D), with narrow leaves that apparently lacked their petioles (Fig. 1D, E) and a dwarf and compact inflorescence with minute, apparently filamentous, flowers (Fig. 1D, E). Due to their tiny size and the delicate, filamentous appearance of their inflorescences, we named this mutant *moss*.

The moss *mutant has dramatic defects in the architecture of its inflorescence*

We analysed in more detail the mutant inflorescence phenotype of *moss* plants (BC_3 line) after being backcrossed three times to L*er*. We observed that the dwarf phenotype of the *moss* plants was partly due to lack of elongation of the internodes between flowers. This caused a dramatic change in the architecture of its inflorescences, which were very compact and resembled an umbel rather than a raceme, the typical inflorescence of wild-type arabidopsis (Fig. 1C, E) (Weberling, 1992; Benlloch *et al.*, 2007).

In the *moss* inflorescences, filamentous organs were seen in the inflorescence stem and in floral pedicels (Fig. 1E, H). Because they were green and frequently located at the base of the lateral inflorescences and of flowers, they might represent modified cauline leaves and bracts. Flowers of the *moss* mutant also exhibited severe alterations (Fig. 1G, H). The number of floral organs was reduced, petals and stamens were replaced by filamentous organs, and carpels were unfused; *moss* flowers were, consequently, sterile.

Finally, a conspicuous inflorescence phenotype in the *moss* plants was an increased number of coflorescences. The number of rosette leaves of moss mutant plants was essentially the same as in the wild-type plants, but the number of coflorescences produced by *moss* plants was about 2-fold more than that of the wild type (Table 1; Fig. 1E, F).

The moss *mutant has increased and ectopic expression of* TFL1

As explained above, besides its defects in plant architecture, the *moss* mutant was selected because of its increased and ectopic expression of the *TFL1::GUS* reporter, which prompted us to study *TFL1* expression in more detail in the *moss* mutant.

We analysed the expression of *TFL1::GUS* in the shoot apex during development (Fig. 2A). The analysis was performed with plants derived from the *moss* BC_3 line that had lost the original pBTG1 reporter and where the reporter pBTG6 was introduced. The pBTG6 reporter construct is essentially identical to pBTG1 but contains the complete *TFL1* 3′ intergenic region (approx. 3·7 kb; Supplementary Data Fig. S1) and, thus, it reproduces the expression of the endogenous *TFL1* gene more accurately. In *moss* pBTG6 plants, the expression of *TFL1::GUS* was stronger in the SAM both in the vegetative and in the inflorescence phases, becoming ectopic in the flowers of the mutant in the adult inflorescence (Fig. 2A).

We also analysed by RT-qPCR the expression of the endogenous *TFL1* gene in adult inflorescence apices. The level of *TFL1* mRNA was clearly higher in *moss* than in the wild type (Fig. 2B), indicating that the altered *TFL1::GUS* expression observed indeed reflects a stronger expression of the endogenous *TFL1* gene in the mutant.

In F_2 plants derived from backcrosses of *moss* to the parental wild type, all the plants with altered *TFL1::GUS* expression showed the characteristic *moss* plant architecture. This indicates that the plant architecture defects and the altered *TFL1* expression are two aspects of the pleiotropic phenotype caused by the *moss* mutation and suggests that the gene mutated in *moss* regulates both *TFL1* expression and plant architecture.

The moss *phenotype is caused by a hypomorphic mutation in* AGO1

We followed a positional cloning approach to identify the gene responsible for the *moss* plant architecture mutant phenotype. The *moss* mutation was mapped to a 16 kb candidate region of

TABLE 1. *Plant architecture of mutants*

Genotype	Rosette leaves*	Cauline leaves[†]	Total leaves[‡]	Coflorescences[§]	Axillary flowers[¶]	Terminal flower**
L*er*	6·73 ± 0·23	2·93 ± 0·12	9·67 ± 0·21	2·90 ± 0·12	ND	−
moss	6·27 ± 0·17	3·07 ± 0·38[††]	9·33 ± 0·46	5·91 ± 0·34	ND	−
tfl1-2	5·60 ± 0·13	2·33 ± 0·19	7·93 ± 0·15	0·20 ± 0·14	2·13 ± 0·17	+
moss tfl1-2	6·27 ± 0·45	0·73 ± 0·15	7·00 ± 0·50	0·13 ± 0·09	0·73 ± 0·15[‡‡]	+
Col	8·6 ± 016	2·4 ± 016	11·0 ± 021	2·4 ± 016	ND	−
ago1-26	8·9 ± 028	7·4 ± 037	16·3 ± 0·6	7·4 ± 037	ND	−
tfl1-1	5·80 ± 0·31	1·80 ± 0·15	7·60 ± 0·38	0·00 ± 0·00	1·80 ± 0·15	+
ago1-26 tfl1-1	4·56 ± 0·29	3·67 ± 0·58	8·22 ± 0·83	0·56 ± 0·29	3·11 ± 0·61	+

Data are means ± standard error ($n \geq 12$).
ND, not detected.
*Number of rosette leaves.
[†]Number of cauline leaves in the main inflorescence stem.
[‡]Number of rosette leaves + cauline leaves.
[§]Number of coflorescences in the main inflorescence stem.
[¶]Number of axillary flowers in the main inflorescence stem.
**Presence (+) or absence (−) of a terminal flower at the inflorescence apex.
[††]The number of cauline leaves in *moss* mutant genotypes might be underestimated, because, apparently, some of them are were transformed into filaments.
[‡‡]Because the number of cauline leaves in *moss* mutant genotypes might be underestimated, the number of axillary flowers in *moss tfl1-2* might be underestimated.

chromosome 1 (Fig. 3A). This region encompass 26 annotated genes; one of these genes is *AGO1*, which encodes a pivotal component of the RNA silencing machinery (Vaucheret *et al.*, 2004; Baumberger and Baulcombe, 2005; Qi *et al.*, 2005). We observed that the inflorescence of the *moss* mutant resembled that of an *ago1 fil yab* triple mutant previously reported (Yang *et al.*, 2006), which suggested that the *moss* mutation could map to the *AGO1* gene. Sequencing of the *AGO1* gene from the *moss* mutant identified a point mutation in the first nucleotide of the 18nth exon (G to A) that causes the replacement of a highly conserved glycine by aspartate in the PIWI domain of the AGO1 protein (Fig. 3B, C); the PIWI domain is required for the cleavage of target mRNAs (Cerutti *et al.*, 2000; Liu *et al.*, 2004; Song *et al.*, 2004).

To test whether this mutation in the *AGO1* gene was responsible for the *moss* plant architecture phenotype, we performed an allelism test by crossing heterozygous *moss/+* plants with plants homozygous for *ago-52*, a hypomorphic mutation causing a phenotype less severe than that of the *moss* mutant (Jover-Gil *et al.*, 2012). One half of the resulting F_1 progeny exhibited a wild-type phenotype (21 out of 45 F_1 plants analysed), whereas the rest of the plants had a phenotype similar to that of the homozygous *ago1-52* parent (Fig. 3D). This result demonstrates that the *moss* mutation and *ago1-52* are allelic and that the architecture phenotype of *moss* plants is caused by the mutation in *AGO1*. Therefore, the *moss* mutant was called *ago1-103* and hereafter we refer to *moss* as *moss/ago1-103*.

Reduction of AGO1 function causes ectopic expression of TFL1

To address whether the phenotype of increased ectopic expression of *TFL1* observed in the *moss/ago1-103* mutant was also due to the mutation in *AGO1*, we tested whether *TFL1* expression was also altered in other *ago1* mutants.

We studied *ago1-26*, another hypomorphic *ago1* allele with a mutation causing the substitution of a conserved amino acid also in the PIWI domain (Morel *et al.*, 202). The *ago1-26* mutant exhibited a morphological phenotype that included: slight reduction in plant size; alteration in the shape of leaves, which had serrated blade margins and were narrow and apparently without petioles (Figs 4A, B and 5E, G); and flowers with reduced fertility, although with apparently normal organs. All these traits resembled those of *moss/ago1-103*, although they were milder in severity. In contrast to *moss/ago1-103*, in the inflorescences of *ago1-26* mutant plants cauline leaves were not transformed into filaments, and flowers were separated by elongated internodes (Figs 4B and 5G). Nevertheless, *ago1-26* plants had a larger number of coflorescences than its wild-type parent (Col) although it produced a similar number of rosette leaves (Table 1; Figs 4A, B and 5E, G). This aspect of the *ago1-26* inflorescence phenotype is similar to that of *moss/ago1-103*, which indicates that an increase in the number of coflorescences is indeed a characteristic trait of *ago1* mutants.

To analyse the effect of the *ago1-26* mutation on *TFL1* expression, we introgressed the *TFL1::GUS* construct pBTG6 into *ago1-26*. As seen in *moss/ago1-103*, ectopic *TFL1::GUS* expression was observed in *ago1-26* flowers (Fig. 4C, D).

Our observation that two independent *ago1* mutants exhibit proliferation of coflorescences and ectopic *TFL1* expression indicates that both traits are caused by the *ago1* mutations and that *AGO1* regulates both the expression of *TFL1* and inflorescence architecture.

Proliferation of coflorescences in ago *mutants is mediated by* TFL1

It has been previously shown that high constitutive expression of *TFL1* in *35S::TFL1* arabidopsis plants leads to a strong increase in the number of coflorescences (Ratcliffe *et al.*, 1998). Therefore, the proliferation of coflorescences observed in the *moss/ago1-103* and *ago1-26* mutants might be due to their increased ectopic *TFL1* expression. To assess this hypothesis, we generated *moss/ago1-103 tfl1-2* and *ago1-26 tfl1-1* double mutants, to test whether the lack of *TFL1* function led to a reduction in the number of coflorescences in the *ago1* mutants. Other aspects of the *ago1* mutant phenotype, such as the floral defects or the lack of internode elongation between flowers (in *moss/ago1-103*), were not suppressed in the *ago1 tfl1* double mutants.
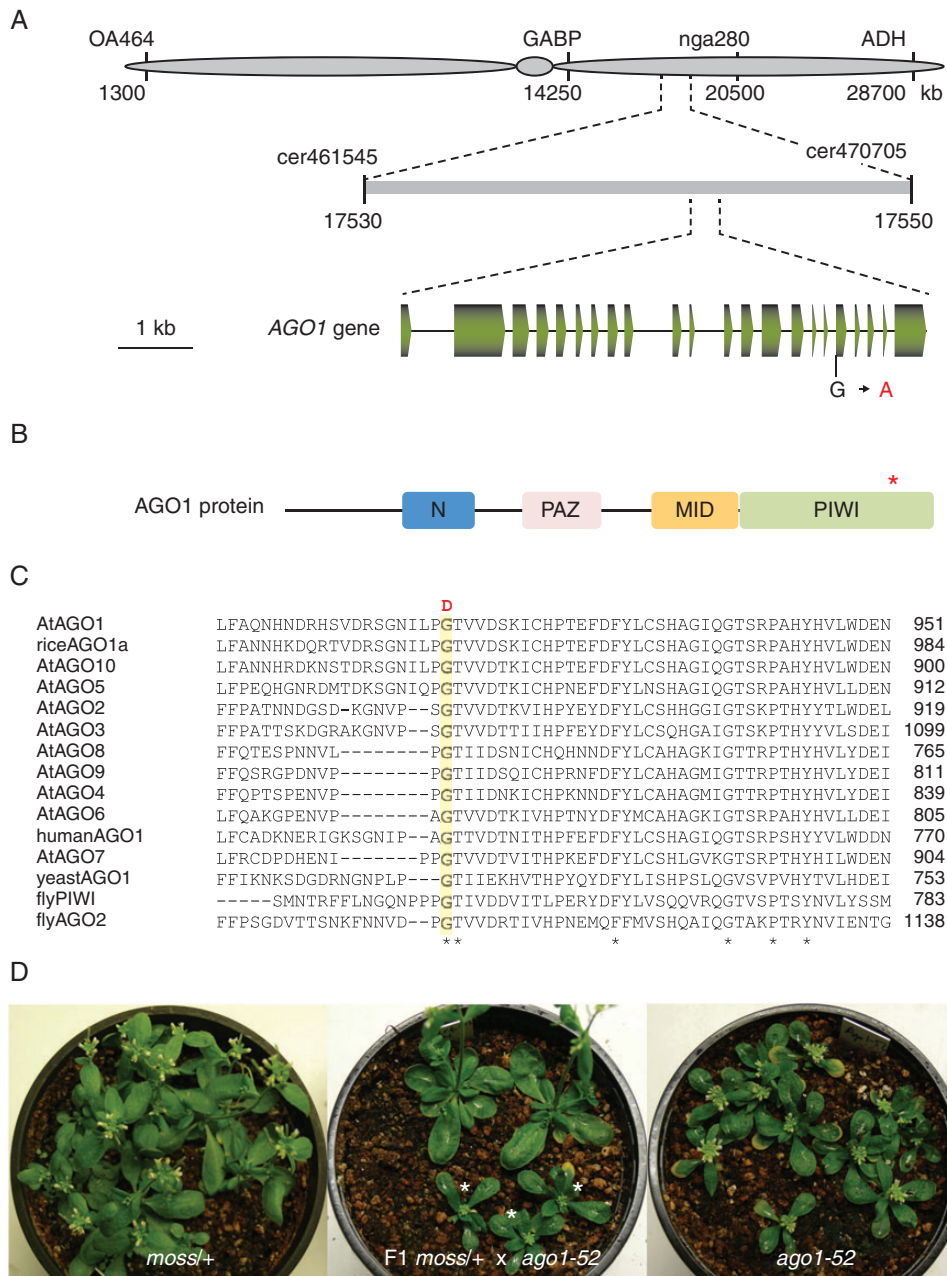
FIG. 3. Cloning of the *moss* mutation. (A) Positional cloning of the *moss* mutation. Some of the markers used for linkage analysis are shown. (B) Schematic representation of the structure of the AGO1 protein, with indication of the N, PAZ, MID and PIWI domains. An asterisk indicates the position of the amino acid affected by the *moss* mutation. (C) Multiple alignment of the region of the arabidopsis AGO1 protein [AtAGO1 (O04379)] affected by the *moss* mutation with those of other AGO family members from *Arabidopsis thaliana* [AtAGO2 (Q9SHF3), AtAGO3 (Q9SHF2), AtAGO4 (Q9ZVD5), AtAGO5 (Q9ZVD5), AtAGO6 (O48771), AtAGO6 (Q9C793), AtAGO8 (Q3E984), AtAGO9 (Q84VQ0) and AtAGO10 (9XGW1)], *Oryza sativa* [riceAGO1a (Q6EU14)], *Homo sapiens* [humanAGO1 (Q9UL18)], *Saccharomyces pombe* [yeastAGO1 (O74957)] and *Drosophila melanoganster* [flyPIWI (Q9VKM1) and flyAGO2 (Q9VUQ5)]. Amino acid residues conserved in all the sequences are marked with an asterisk. The residue changed by the mutation in the *moss* mutant (G-D), shaded in yellow, is conserved in all the protein sequences. (D) *moss/AGO1* heterozygotes (left), *ago1-52/ago1-52* homozygotes (right) and their F_1 progeny (centre), among which *moss/ago1-52* heterozygotes segregated in a 1:1 (phenotypically mutant:wild-type) ratio. The latter was considered evidence of allelism.

The *tfl1* mutations partly suppressed the inflorescence architecture observed in *ago1* mutants; a drastic decrease in the number of vegetative leaves and coflorescences was observed in *moss/ago1-103 tfl1-2* and *ago1-26 tfl1-1* compared with their *ago1* parents (Table 1; Fig. 5).

These results show that *TFL1* mediates the increased production of coflorescences of *ago1* mutants and indicate that AGO1 controls inflorescence architecture in part through the regulation of *TFL1* expression.

DISCUSSION

In this paper we describe our work to identify regulators of *TFL1* through a genetic screening for mutants with altered *TFL1*
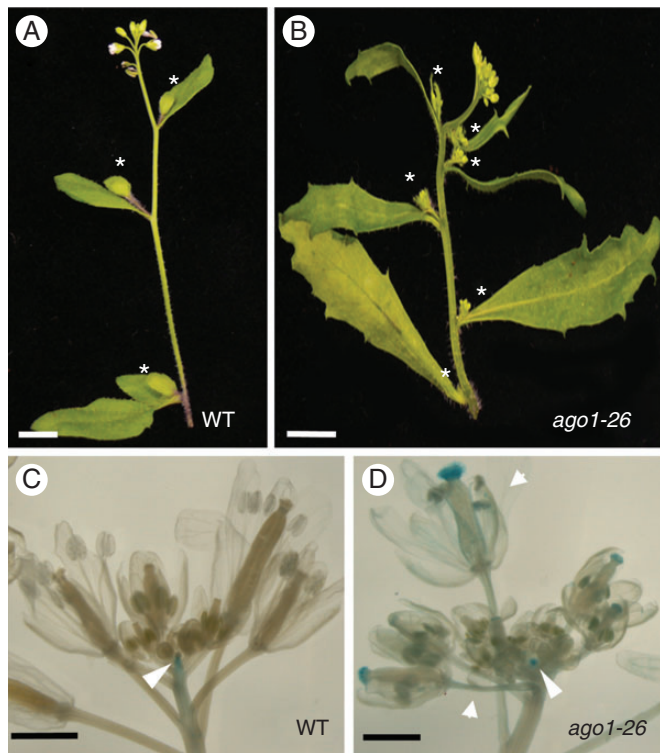
FIG. 4. Inflorescence phenotype of the *ago1-26* mutant. (A) Main inflorescence of a Col wild-type (WT) plant, with three coflorescences (asterisks). (B) Main inflorescence of an *ago1-26* mutant plant, with six coflorescences. (C) Expression of *TFL1::GUS* in the inflorescence apex of a Col WT plant. GUS signal is restricted to the inflorescence meristem (arrowhead). (D) Expression of *TFL1::GUS* in the inflorescence apex of an *ago1-26* mutant plant. GUS signal is observed not only in the inflorescence meristem (arrowhead) but also in the flowers, in the floral organs and in the pedicels (arrows). Scale bars: 5 mm in (A) and (B); 1 mm in (C) and (D).

expression. Our results show that AGO1 acts as a repressor of *TFL1* expression and reveal a novel role for AGO1 as a regulator of inflorescence architecture. Our study provides evidence supporting that AGO1 contributes to the control of inflorescence architecture through its activity as a regulator of *TFL1* expression.

Several studies involving the characterization of *ago1* mutants have shown that *AGO1* participates in the regulation of key developmental processes in arabidopsis (Jover-Gil *et al.*, 2005; Kidner and Martienssen, 2005*b*; Zhang and Zhang, 2012). A large number of independent *ago1* mutants have been described that show diverse phenotypes, ranging from hardly viable null alleles causing severe developmental defects (Bohmert *et al.*, 1998; Kidner and Martienssen, 2004), to fully fertile hypomorphic alleles with only mild defects (Morel *et al.*, 2002; Jover-Gil *et al.*, 2012). Nevertheless, essentially all *ago1* mutants show pleitropic phenotypes, which is consistent with the central role of *AGO1* in miRNA-mediated gene silencing, a process that regulates the expression of a large number of genes (Vaucheret *et al.*, 2004). Though *moss/ago1-103* is a hypomorphic mutation that still allows development of a plant with a 'complete' inflorescence, the *moss/ago1-103* plants show severe developmental defects. This is most probably due to the fact that the *moss/ago1-103* mutation causes the substitution of a highly

conserved amino acid in the C-terminal region of the AGO1 protein, possibly leading to a protein where the activity of the PIWI domain, required for the cleavage of mRNAs that are targeted by miRNAs (Cerutti *et al.*, 2000; Liu *et al.*, 2004; Song *et al.*, 2004), is severely compromised.

AGO1 is involved in a wide variety of developmental processes. Thus, it participates in the control of general processes that affect the development of all aerial plant organs, such as organ polarity and the functioning of stem cells in the shoot meristems (Kidner *et al.*, 2004), but it is also involved in other more specific processes. For instance, in leaf development, it plays a role in the growth of the lamina and in the venation patterning (Palatnik *et al.*, 2003; Jover-Gil *et al.*, 2012). In reproductive development, AGO1 has been shown to be involved in processes such as meristem identity and in the termination of floral stem cells (Kidner and Martienssen, 2005*a*; Ji *et al.*, 2011). However, AGO1 does not seem to be involved in other important processes in reproductive development such as, for instance, the floral transition (measured as the number of rosette leaves), as indicated by the study of Kidner and Martienssen (2005*a*) and by our own results. In most cases, it has been shown that AGO1 affects these processes by regulating the expression of transcription factors that are key developmental regulators (Jover-Gil *et al.*, 2005; Kidner and Martienssen, 2005*b*; Zhang and Zhang, 2012).

Our study reveals a novel role for AGO1 in reproductive development, controlling inflorescence architecture. Thus, both in *moss/ago1-103* and in *ago1-26* the first inflorescence phase (I1) is enlarged, with an increase in the number of coflorescences produced. Our results indicate that this phenotype, which resembles the effect of *TFL1* overexpression in *35S::TFL1* transgenic plants, with a very enlarged I1 phase, is due to the misexpression of *TFL1* in the *ago1* mutants. Moreover, suppression of proliferation of coflorescences in *ago1 tfl1* double mutants indicates that this proliferation requires the activity of *TFL1* and supports that this role of AGO1 in the regulation of inflorescence architecture is based on its activity as a repressor of *TFL1* expression.

Though *moss/ago1-103* has an increased number of coflorescences, it does produce the same number of rosette leaves as the wild type. This is in contrast to what occurs in *35::TFL1* but it is what is observed in other *ago1* mutants (*ago1-26*, this study; Kidner and Martienssen, 2004). The similar length of the rosette leaves phase in *moss/ago1-103* and the wild type might be due to the fact that the level of *TFL1* expression in that phase in *moss/ago1-103* is quite moderate, while in the early inflorescence apex it is much higher. It does not seem surprising that in the rosette leaves phase the phenotype of *moss/ago1-103* differs from that of *35::TFL1*, where expression of *TFL1* is strong and constitutive.

How does AGO1 repress *TFL1* expression? One possibility would be that *TFL1* expression was controlled by post-transcriptional gene silencing, the *TFL1* transcript being a target of miRNA-guided degradation or translational arrest, mediated by AGO1. This is the case for several key developmental regulators such as some members of the TCP transcription factor family involved in leaf morphology (Palatnik *et al.*, 2003) or the HD-ZIP III transcription factors involved in leaf polarity (Kidner and Martienssen, 2004). However, it seems unlikely that miRNA-mediated gene silencing is the cause of the misregulation of *TFL1* expression in the *ago1* mutants.
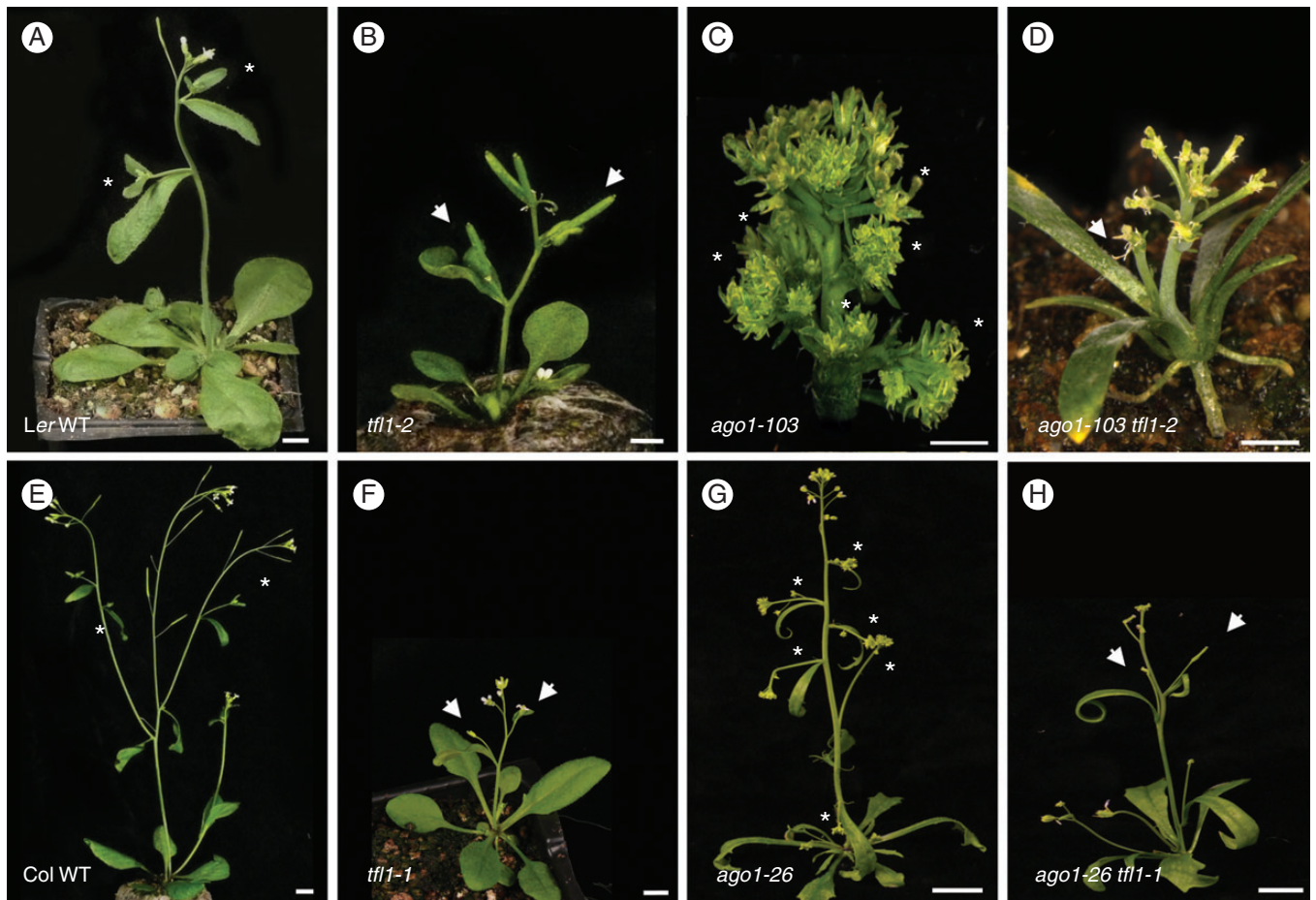
Fig. 5. Phenotype of *ago1 tfl1* double mutants. (A) A Landsberg *erecta* (L*er*) wild-type (WT) plant, with a main inflorescence with two coflorescences (asterisks). The *tfl1-2* and *moss* mutants are in a L*er* genetic background. (B) A *tfl1-2* mutant plant. Instead of coflorescences, its main inflorescence has two axillary flowers (arrows). (C) Main inflorescence of a *moss/ago1-103* mutant plant, with six coflorescences (asterisks). (D) A *moss/ago1-103 tfl1-2* double mutant plant. Instead of coflorescences, its main inflorescence has one axillary flower (arrow). (E) A Columbia (Col) WT plant, with a main inflorescence with two coflorescences (asterisks). The genetic background of the *tfl1-1* and *ago1-26* mutants is Col. (F) A *tfl1-1* mutant plant. Instead of coflorescences, its main inflorescence has two axillary flowers (arrows). (G) An *ago1-26* mutant plant, with a main inflorescence with six coflorescences (asterisks). (H) An *ago1-26 tfl1-1* double mutant plant. Instead of coflorescences, its main inflorescence has two axillary flowers (arrows). Scale bars: 5 mm.

Thus, though the *TFL1* genomic fragments in pBTG1 (the reporter construct in the line used in the mutagenesis; Supplementary Data Fig. S1) only contain a very small part of the *TFL1* transcribed sequence, the 5′UTR, the *moss/ago1-103* mutant still showed high ectopic expression of the *TFL1::GUS* transgene from pBTG1 (Fig. 1B). The 5′UTR of *TFL1* is only 45 nucleotides long (A. Serrano-Mislata and F. Madueño, IBMCP, Valencia, Spain, unpubl. res.), and in the analysis of that sequence we did not identify any predicted target site for miRNAs. Therefore, this strongly indicates that AGO1 regulation does not regulate *TFL1* expression by directly acting on its transcript

Alternatively, AGO1 might be indirectly involved in the repression of *TFL1*, acting on other direct regulators of *TFL1*. The floral identity genes *AP1* and *LFY* encode transcription factors that directly bind to sequences in the regulatory region of *TFL1* (Kaufmann *et al.*, 2010; Moyroud *et al.*, 2011; Winter *et al.*, 2011), and are required to repress its expression in the flower (Ratcliffe *et al.*, 1999; Liljegren *et al.*, 1999; Bowman *et al.*, 1993; Ferrándiz *et al.*, 2000; Parcy *et al.*, 2002). The inflorescence phenotype of *ago1* mutants somehow resembles that of loss-of-function alleles of *AP1* and *LFY*, which also have an increased number of coflorescences, because the most basal flowers in their inflorescences are replaced by inflorescence-like structures (Schultz and Haugh, 1991; Mandel *et al.*, 1992; Weigel *et al.*, 1992; Bowman *et al.*, 1993). As reported by Kidner and Martienssen (2005*a*), the expression of *AP1* and *LFY* is downregulated in *ago1* mutants. Therefore, a likely possibility is that the low levels of *AP1* and *LFY* in *ago1* mutants lead to the increased expression of *TFL1*, ectopic in flowers, and to the proliferation of coflorescences. Because *AP1* and *LFY* do not seem to be direct targets of miRNA-mediated regulation either, it might possibly be necessary to look for factors upstream of *AP1* and *LFY* to understand fully how AGO1 regulates *TFL1* expression.

SUPPLEMENTARY DATA

Supplementary data are available online at www.aob.oxford journals.org and consist of the following. Figure S1: reporter TFL1::GUS constructs. Table S1: list of primers used in this study.

ACKNOWLEDGEMENTS

LITERATURE CITED

Abe M, Kobayashi Y, Yamamoto S, *et al.* 2005. A bZIP protein mediating signals from the floral pathway integrator FT at the shoot apex. *Science* **309**: 1052–1056.

Ahn JH, Miller D, Winter VJ, *et al.* 2006. A divergent external loop confers antagonistic activity on floral regulators FT and TFL1. *EMBO Journal* **25**: 605–614.

Alvarez J, Guli C, Yu X, Smyth D. 1992. *TERMINAL FLOWER1*: a gene affecting inflorescence development in Arabidopsis thaliana. *The Plant Journal* **2**: 103–116.

Amasino R. 2010. Seasonal and developmental timing of flowering. *The Plant Journal* **61**: 1001–1013.

Andres F, Coupland G. 2012. The genetic basis of flowering responses to seasonal cues. *Nature Reviews Genetics* **13**: 627–639.

Baulcombe DC. 2004. RNA silencing in plants. *Nature* **431**: 356–363.

Bartel DP. 2009. MicroRNAs: target recognition and regulatory functions. *Cell* **136**: 215–233.

Baumberger N, Baulcombe DC. 2005. Arabidopsis ARGONAUTE1 is an RNA Slicer that selectively recruits rnicroRNAs and short interfering RNAs. *Proceedings of the National Academy of Sciences, USA* **102**: 11928–11933.

Benlloch R, Berbel A, Serrano-Mislata A, Madueno F. 2007. Floral initiation and inflorescence architecture: a comparative view. *Annals of Botany* **100**: 659–676.

Bevan M. 1994. Binary *Agrobacterium* vectors for plant transformation. *Nucleic Acids Research* **12**: 8711–8721.

Blázquez MA, Ferrándiz C, Madueno F, Parcy F. 2006. How floral meristems are built. *Plant Molecular Biology* **60**: 855–870.

Bohmert K, Camus I, Bellini C, Bouchez D, Caboche M, Benning C. 1998. *AGO1* defines a novel locus of *Arabidopsis* controlling leaf development. *EMBO Journal* **17**: 170–180.

Bowman J, Alvarez J, Weigel D, Meyerowitz E. 1993. Control of flower development in Arabidopsis thaliana by *APETALA1* and interacting genes. *Development* **119**: 721–743.

Bowman J. 1994. *Arabidopsis: an atlas of morphology and development*. New York: Springer-Verlag.

Bradley DJ, Ratcliffe O, Vincent C, Carpenter R, Coen E. 1997. Inflorescence commitment and architecture in Arabidopsis. *Science* **275**: 80–83.

Brodersen, Voinnet O. 2009. Revisiting the principles of microRNA target recognition and mode of action. *Nature Reviews Molecular Cell Biology* **10**: 141–148.

Carthew RW, Sontheimer EJ. 2009. Origins and mechanisms of miRNAs and siRNAs. *Cell* **136**: 642–655.

Cerutti L, Mian N, Bateman A. 2000. Domains in gene silencing and cell differentiation proteins: the novel PAZ domain and redefinition of the Piwi domain. *Trends in Biochemical Sciences* **25**: 481–482.

Conti L, Bradley DJ. 2007. TERMINAL FLOWER1 is a mobile signal controlling Arabidopsis architecture. *The Plant Cell* **19**: 767–778.

Czechowski T, Stitt M, Altmann T, Udvardi MK, Scheible W-R. 2005. Genome-wide identification and testing of superior reference genes for transcript normalization in Arabidopsis. *Plant Physiology* **139**: 5–17.

Ferrándiz C, Gu Q, Martienssen RA, Yanofsky MF. 2000. Redundant regulation of meristem identity and plant architecture by *FRUITFULL*, *APETALA1* and *CAULIFLOWER*. *Development* **127**: 725–734.

Griffiths-Jones S. 2004. The microRNA Registry. *Nucleic Acids Research* **32**: D109–D111.

Griffiths-Jones S, Grocock RJ, van Dongen S, Bateman A, Enright AJ. 2006. miRBase: microRNA sequences, targets and gene nomenclature. *Nucleic Acids Research* **34**: D140–D144.

Griffiths-Jones S, Saini HK, van Dongen S, Enright AJ. 2008. miRBase: tools for microRNA genomics. *Nucleic Acids Research* **36**: D154–D158.

Hanano S, Goto K. 2011. Arabidopsis *TERMINAL FLOWER1* is involved in the regulation of flowering time and inflorescence development through transcriptional repression. *The Plant Cell* **23**: 3172–3184.

Hanzawa Y, Money T, Bradley D. 2005. A single amino acid converts a repressor to an activator of flowering. *Proceedings of the National Academy of Sciences, USA* **102**: 7748–7753.

Ho WW, Weigel D. 2014. Structural features determining flower-promoting activity of Arabidopsis FLOWERING LOCUS T. *The Plant Cell* **26**: 552–564.

Huijser P, Schmid M. 2011. The control of developmental phase transitions in plants. *Development* **138**: 4117–4129.

Jefferson RA, Kavanagh TA, Bevan MW. 1987. GUS fusions: beta-glucuronidase as a sensitive and versatile gene fusion marker in higher plants. *EMBO Journal* **6**: 3901–3907.

Ji L, Liu X, Yan J, *et al.* 2011. ARGONAUTE10 *and* ARGONAUTE1 *regulate the termination of floral stem cells through two microRNAs in arabidopsis*. *PLoS Genetics* **7**: e1001358.

Jover-Gil S, Candela H, Ponce MR. 2005. Plant microRNAs and development. *International Journal of Developmental Biology* **49**: 733–744.

Jover-Gil S, Candela H, Robles P, *et al.* 2012. The microRNA pathway genes *AGO1*, *HEN1* and *HYL1* participate in leaf proximal–distal, venation and stomatal patterning in Arabidopsis. *Plant and Cell Physiology* **53**: 1322–1333.

Kaufmann K, Wellmer F, Muiño JM, *et al.* 2010. Orchestration of floral initiation by *APETALA1*. *Science* **328**: 85–89.

Kidner CA, Martienssen RA. 2004. Spatially restricted microRNA directs leaf polarity through ARGONAUTE1. *Nature* **428**: 81–84.

Kidner CA, Martienssen RA. 2005a. The role of *ARGONAUTE1* (*AGO1*) in meristem formation and identity. *Developmental Biology* **280**: 504–517.

Kidner CA, Martienssen RA. 2005b. The developmental role of microRNA in plants. *Current Opinion in Plant Biology* **8**: 38–44.

Kozomara A, Griffiths-Jones S. 2014. miRBase: annotating high confidence microRNAs using deep sequencing data. *Nucleic Acids Research* **42**: D68–D73.

Liljegren SJ, Gustafson-Brown C, Pinyopich A, Ditta G, Yanofsky MF. 1999. Interactions among *APETALA1*, *LEAFY*, and *TERMINAL FLOWER1* specify meristem fate. *The Plant Cell* **11**: 1007–1018.

Liu C, Teo ZWN, Bi Y, *et al.* 2013. A conserved genetic pathway determines inflorescence architecture in Arabidopsis and rice. *Developmental Cell* **24**: 612–622.

Liu J, Carmell MA, Rivas FV, *et al.* 2004. Argonaute2 is the catalytic engine of mammalian RNAi. *Science* **305**: 1437–1441.

Mandel MA, Gustafson-Brown C, Savidge B, Yanofsky MF. 1992. Molecular characterization of the Arabidopsis floral homeotic gene *APETALA1*. *Nature* **360**: 273–277.

Morel J-B, Godon C, Mourrain P, *et al.* 2002. Fertile hypomorphic *ARGONAUTE* (*ago1*) mutants impaired in post-transcriptional gene silencing and virus resistance. *The Plant Cell* **14**: 629–639.

Moyroud E, Minguet EG, Ott F, *et al.* 2011. Prediction of regulatory interactions from genome sequences using a biophysical model for the Arabidopsis LEAFY transcription factor. *The Plant Cell* **23**: 1293–1306.

Palatnik J, Allen E, Wu X, *et al.* 2003. Control of leaf morphogenesis by microRNAs. *Nature* **425**: 257–263.

Parcy F, Bomblies K, Weigel D. 2002. Interaction of *LEAFY*, *AGAMOUS* and *TERMINAL FLOWER1* in maintaining floral meristem identity in Arabidopsis. *Development* **129**: 2519–2527.

Ponce MR, Robles P, Lozano FM, Brotóns MA, Micol JL. 2006. Low-resolution mapping of untagged mutations. *Methods in Molecular Biology* **323**: 105–113.

Prusinkiewicz P, Erasmus Y, Lane B, Harder LD, Coen E. 2007. Evolution and development of inflorescence architectures. *Science* **316**: 1452–1456.

Qi Y, Denli AM, Hannon GJ. 2005. Biochemical specialization within Arabidopsis RNA silencing pathways. *Molecular Cell* **19**: 421–428.

Ratcliffe OJ, Amaya I, Vincent CA, *et al.* 1998. A common mechanism controls the life cycle and architecture of plants. *Development* **125**: 1609–1615.

Ratcliffe OJ, Bradley DJ, Coen E. 1999. Separation of shoot and floral identity in Arabidopsis. *Development* **126**: 1109–1120.

Rusinov V, Baev V, Minkov IN, Tabler M. 2005. MicroInspector: a web tool for detection of miRNA binding sites in an RNA sequence. *Nucleic Acids Research* **33**: 696–700.

Schmittgen TD, Livak KJ. 2008. Analyzing real-time PCR data by the comparative C(T) method. *Nature Protocols* **3**: 1101–1108.

Schultz E, Haughn GW. 1991. *LEAFY*, a homeotic gene that regulates inflorescence development in Arabidopsis. *The Plant Cell* **3**: 771–781.

Shannon S, Meeks-Wagner D. 1991. A mutation in the Arabidopsis *TFL1* gene affects inflorescence meristem development. *The Plant Cell* **3**: 877–892.

Shannon S, Meeks-Wagner D. 1993. Genetic interactions that regulate inflorescence development in Arabidopsis. *The Plant Cell* **5**: 639–655.

Smith MR, Willmann MR, Wu G, *et al.* **2009.** Cyclophilin 40 is required for microRNA activity in Arabidopsis. *Proceedings of the National Academy of Sciences, USA* **106**: 5424–5429.

Sohn EJ, Rojas-Pierce M, Pan S, *et al.* **2007.** The shoot meristem identity gene *TFL1* is involved in flower development and trafficking to the protein storage vacuole. *Proceedings of the National Academy of Sciences, USA* **104**: 18801–18806.

Song J-J, Smith SK, Hannon GJ, Joshua-Tor L. 2004. Crystal structure of Argonaute and its implications for RISC slicer activity. *Science* **305**: 1434–1437.

Teo ZWN, Song S, Wang Y-Q, Liu J, Yu H. 2013. New insights into the regulation of inflorescence architecture. *Trends in Plant Science* **19**: 158–165.

Vaucheret H. 2006. Post-transcriptional small RNA pathways in plants: mechanisms and regulations. *Genes and Development* **20**: 759–771.

Vaucheret H, Vazquez F, Crété P, Bartel DP. 2004. The action of ARGONAUTE1 in the miRNA pathway and its regulation by the miRNA pathway are crucial for plant development. *Genes and Development* **18**: 1187–1197.

Weberling F. 1992. *Morphology of flowers and inflorescences.* Cambridge: Cambridge University Press.

Weigel D, Glazebrook J. 2002. *Arabidopsis: a laboratory manual.* Cold Spring Harbor, NY: Cold Spring Harbor Laboratory Press.

Weigel D, Alvarez JP, Smyth DR, Yanofsky MF, Meyerowitz EM. 1992. *LEAFY* controls floral meristem identity in Arabidopsis. *Cell* **69**: 843–859.

Wigge PA, Kim MC, Jaeger KE, *et al.* **2005.** Integration of spatial and temporal information during floral induction in arabidopsis. *Science* **309**: 1056–1059.

Winter CM, Austin RS, Blanvillain-Baufumé S, *et al.* **2011.** *LEAFY* target genes reveal floral regulatory logic, cis motifs, and a link to biotic stimulus response. *Developmental Cell* **20**: 430–443.

Wolpert L, Tickle C. 2010. *Principles of development.* Oxford: Oxford University Press.

Yang L, Wang H, Xu Y, Huang H. 2006. Characterizations of a hypomorphic argonaute1 mutant reveal novel AGO1 functions in Arabidopsis lateral organ development. *Plant Molecular Biology* **61**: 63–78.

Zhang Z, Zhang X. 2012. Argonautes compete for miR165/166 to regulate shoot apical meristem development. *Current Opinion in Plant Biology* **15**: 1–7.

SUPPLEMENTARY DATA

Figure S1. Reporter *TFL1::GUS* constructs. (A) Diagram of the genomic region encompassing the *TFL1* gene. The *TFL1* gene and the flanking open reading frames are represented by light blue boxes, and the intergenic regions by a grey line. In the *TFL1* gene, the 5' and 3' untranslated regions (UTRs) are represented by white boxes. (B) Diagram of the pBTG1 construct. In pBTG1, the *GUS* gene is flanked, in its 5', by a DNA fragment including the complete 5' intergenic region and the *TFL1* 5' UTR (2172 bp) and, in its 3', by a DNA fragment including part of the *TFL1* 3' intergenic region (2722 bp, starting downstream the *TFL1* 3' UTR - i.e., pBTG1 does not contain the *TFL1* 3' UTR). (C) Diagram of the pBTG6 construct. In pBTG6, the *GUS* gene is flanked, in its 5', by a DNA fragment including the complete 5' intergenic region and the *TFL1* 5' UTR (2172 bp) and, in its 3', by a DNA fragment including the complete 3' intergenic region and the *TFL1* 3' UTR (4667 bp).
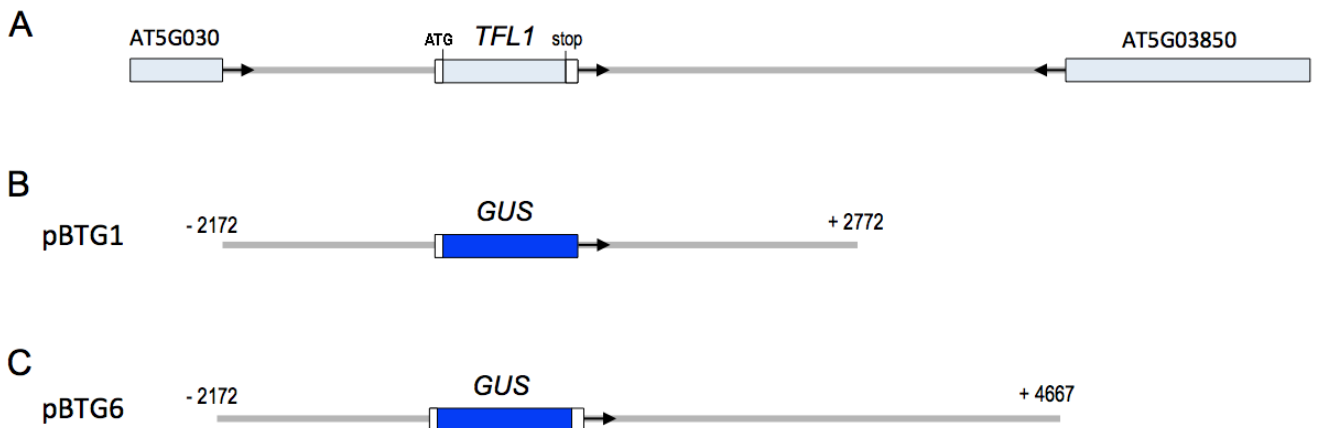
Table S1. List of primers used in this study.

Gene	Purpose	Primer	Sequence
TFL1	5' intergenic region of *TFL1*	TFL15'intF	TGAGTCGACGCTAGGAGATTGTTGATC
TFL1	5' intergenic region of *TFL1*	TFL15'intR	CTGCAGGATCCTTTGTTAACTTAGAGG
TFL1	3' intergenic region of *TFL1*	TFL13'2.7F	GTAGAGCTCTAGAAGTATTGATAACGATCTG TCG
TFL1	3' intergenic region of *TFL1*	TFL13'2.7R	TAGAATTCGGTACCAGAGTCGTTCTAAACCG AAGTATGG
AGO1	Genotyping of the *ago1-26* mutation.	AGOF1	GTATGCAAGATTGTTGAAG
AGO1	Genotyping of the *ago1-52* mutation.	AGOF8	AAATCTGCCACCCTACAGAGTTTG
AGO1	Genotyping of the *ago1-52* mutation.	AGOR6	GTCATAAAGATAGATAGAGGGTG
AGO1	Genotyping of the *ago1-26* mutation.	AGOR8	CCATCCCTGTGCAGAATAACC
AGO1	Genotyping of the *moss/ago1-103* mutation	dCAPmoss-Fw	CATTGGTTTTTAACCCCTTTGTTAATTCTAG
AGO1	Genotyping of the *moss/ago1-103* mutation	dCAPmoss-Rv	AGTAAAGTTGTTCTCATCCCAAAGAACGTG
UBQ10	RT-qPCR	UBQ-Fw	CCTTGTATAATCCCTGATGAATAAGTGT
UBQ10	RT-qPCR	UBQ-Rv	AACAGGAACGGAAACATAGTAGAACA
GUS	RT-qPCR	GUS-Fw	ACCGTACCTCGCATTACCCTT
GUS	RT-qPCR	GUS-Rv	CATCTGCCCAGTCGAGCAT
TFL1	RT-qPCR	TFL1-Fw	AAGCAAAGACGTGTTATCTTTCCTAAT
TFL1	RT-qPCR	TFL1-Rv	GTTGAAGTGATCTCTCGAAGGGAT